Chinese Chemical Letters 33 (2022) 3245–3248

Contents lists available at ScienceDirect

Chinese Chemical Letters

journal homepage: www.elsevier.com/locate/cclet

Biomass-derived dynamic covalent epoxy thermoset with robust mechanical properties and facile malleability

Xiao-Min Ding, Li Chen*, Xi Luo, Feng-Ming He, Yan-Fang Xiao, Yu-Zhong Wang*

The Collaborative Innovation Center for Eco-Friendly and Fire-Safety Polymeric Materials (MoE), National Engineering Laboratory of Eco-Friendly Polymeric Materials (Sichuan), State Key Laboratory of Polymer Materials Engineering, College of Chemistry, Sichuan University, Chengdu 610064, China

ARTICLE INFO

Article history:
Received 20 August 2021
Revised 7 October 2021
Accepted 26 October 2021
Available online 29 October 2021

Keywords:
Epoxy resin
Dynamic covalent thermoset
Protocatechualdehyde
Imine chemistry
High-performance

ABSTRACT

Biomass-derived dynamic covalent thermoset has been considered as a promising solution to the high dependence on fossil resources and the difficulty in recyclability after curing of conventional bisphenol A epoxy resins. However, the design and preparation of a dynamic covalent biobased epoxy thermoset with both comparable thermal and mechanical performances to bisphenol A epoxy resins and reprocessibility remains a significant challenge. Herein, based on imine chemistry, a novel Schiff base-containing dynamic covalent epoxy thermoset was facilely fabricated from biobased protocatechualdehyde and synthetic siloxane diamine. Due to the more reactive epoxides in the epoxy monomer than in bisphenol A epoxy oligomer, the thermoset exhibited a high cross-linking density, resulting in high thermal stability and glass transition temperature. The rigid aromatic Schiff base moieties endowed the thermoset with excellent mechanical properties: Thanks to the plasticization of the flexible siloxane, the thermoset displayed high impact strength. Meanwhile, owing to the high segmental mobility, the fast exchange of imine bonds was guaranteed; and the thermoset was able to be recycled through reprocessing. Taking these features, this work provided great potential for designing and preparing sustainable substitutes for bisphenol A epoxy resins in the high-performance applications.

Epoxy resins (EPs) have become one of the most widely used thermosetting resins and are indispensable in the fields of composite and structural materials, electronics and electricity, coatings and adhesives due to their excellent dimensional stability, adhesive properties, electrical insulation, mechanical properties and corrosion resistance [1–4]. However, about 90% of the EPs currently used are provided from diglycidylether of bisphenol A (DGEBA), which main synthetic raw material bisphenol A (BPA) still largely depends on fossil resources [5]. Meanwhile, BPA is confirmed as hormone disruptor and may pose several threats to the health of life and the ecosystem [6,7]. Moreover, once completely cured, the permanent cross-linking structures of conventional EPs make them difficult to be reprocessed or reused, which results in the waste of resources; and the castoff items from EPs and their fiber reinforced composites that reached their servicing life also cause environmental pollution [8,9]. These problems have become a bottleneck restricting the further development and application of EPs in diverse applications. Therefore, based on renewable resources, the development of malleable and re-processible EPs with comparable comprehensive properties as conventional DGEBA resins is not only resource conservation and environmental protection, but also of practical significance.

Recently, covalent adaptable networks (CANs) have been proposed as an attractive strategy for introducing plasticity into thermosetting resins by introducing reversible bonds [8,10,11], such as non-covalent interactions [12,13] and dynamic covalent bonds (*e.g.*, bonds formed by Diels-Alder reaction [14–16], ester bonds [17–19], boronic ester bonds [20,21], disulfide bonds [22,23], imine bonds [24–26] and coordination bonds [27–29]). The current researches on epoxy CANs show that, due to the reversible dynamic reactions above the transition temperatures, EPs possess excellent self-healing, reshaping, remodeling and recycling capabilities [30–32]. However, in view of the low designability of biobased structures, there are few studies focused on the use of renewable resources to prepare epoxy CANs. Among them, the main two types are Schiff base-containing epoxy CANs based on vanillin [33–35] and anhydride or carboxylic acid cured epoxy CANs based on epoxidized soybean oil [36,37] or other biobased glycidyl ethers [38–41]. Unfortunately, these CANs either have favourable dynamic properties but the comprehensive performances could not meet the requirements of many application fields [24,34,42,43]; or the CANs

* Corresponding authors.
E-mail addresses: l.chen.scu@gmail.com (L. Chen), yzwang@scu.edu.cn (Y.-Z. Wang).

https://doi.org/10.1016/j.cclet.2021.10.079
1001-8417/

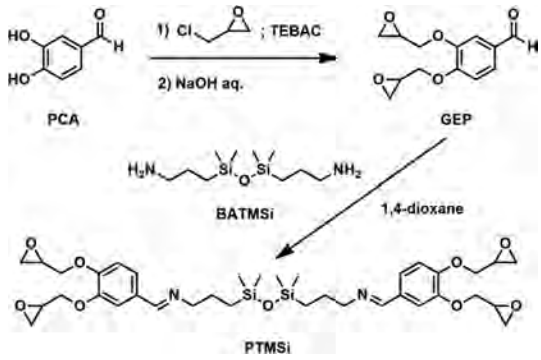

Scheme 1. Synthetic route of PTMSi.

designed based on rigid renewable structures have the thermal and mechanical properties comparable to the conventional DGEBA resins, but network topology rearrangements are restricted by the stiff network and crosslinks, resulting in unsatisfactory malleability [35,44–46].

Herein, we synthesized a novel four-functional Schiff base-containing epoxy monomer (PTMSi) based on the natural aromatic protocatechualdehyde and synthetic siloxane amine. After curing with 4,4′-diaminodiphenylmethane (DDM), a dynamic covalent epoxy thermoset was obtained. Due to the high permanent cross-linking density from the quadruple reactive epoxides, the thermal and mechanical properties of PTMSi/DDM were comprehensively evaluated, and the relevant results were compared with those of conventional DGEBA/DDM. Besides, the dynamic imine bonds were located far from the flexible siloxane units, and the segmental mobility was less hindered by the crosslinks. The malleability of the obtained epoxy thermoset was then carried out.

In order to prevent the formation of benzodioxane derivatives between phenolic compounds with ortho hydroxyl groups and epichlorohydrin [47], the synthesis of PTMSi started from the glycidylation of protocatechualdehyde (PCA). Then the epoxy monomer was obtained through a common aldehyde-amine condensation reaction, as shown in Scheme 1. The relevant structural characterization is shown in Figs. S1–S5 (Supporting information); and the good processability of the liquid epoxy monomer was proved by rheological analysis (Fig. S6 in Supporting information).

The non-isothermal curing behaviors of the two formulations are displayed in Fig. 1, where they reveal similar curing behaviors. All the heating curves were only observed a single curing exothermic peak, which was corresponded to the curing reaction between epoxides and amines. Compared to DGEBA/DDM, the curing exothermic peak shapes of PTMSi/DDM were slightly flat. This was because the curing reaction process with amines became more complicated after the increase of reactive epoxides. As the curing progressed, a large number of permanent crosslinks hindered the probability of effective collisions between secondary amine and epoxides. According to the curing exothermic peak temperature at each heating rate, PTMSi was able to cure with DDM under milder conditions than DGEBA did. Similarly, the curing reaction activation energy (E_a) calculated by Kissinger and Ozawa methods also indicated the high reactivity of PTMSi, and the curing reaction was more likely to occur than conventional epoxy formulation (Fig. 1c). Furthermore, the cured network of PTMSi/DDM was highly complete as its gel content reached more than 99 wt% (Fig. 1d).

Although the temperature of 5 wt% weight loss ($T_{5\%}$) of PTMSi/DDM was slightly lower than that of DGEBA/DDM (Fig. 2a and Table S1 in Supporting information), it was still higher than

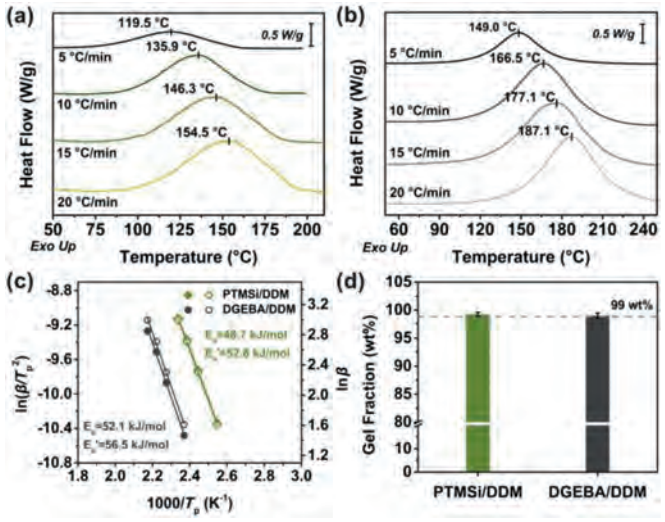

Fig. 1. Evaluation on the curing activity and cured network of epoxy formulation. Non-isothermal DSC thermograms of (a) PTMSi/DDM and (b) DGEBA/DDM with heating rates of 5, 10, 15 and 20 °C/min. (c) Linear fitting plots of $\ln(\beta/T_p^2)$ and $\ln\beta$ against $1/T_p$ based on Kissinger's equation and Ozawa's equation, respectively. (d) The gel fractions of epoxy thermosets.

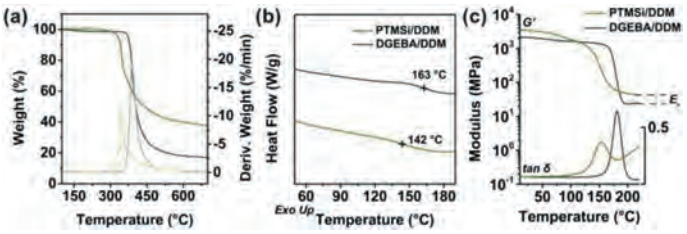

Fig. 2. Thermal properties of PTMSi/DDM and DGEBA/DDM as a comparison. (a) TG and DTG thermographs and (b) DSC curves at a heating rate of 10 °C/min. (c) DMA spectra for the storage modulus (G') and tanδ against temperature at a heating rate of 5 °C/min.

that of the Schiff base-containing EPs reported in the literature [44,45]. The low bonding energy of C=N increased the dissociation tendency at elevated temperatures, resulting in poor $T_{5\%}$ of the thermosets containing imine bonds. As the temperature rose, the decomposition rate of PTMSi/DDM was slow, and finally showed a high residue, which was the result of inert siloxane and cross-linkable aromatic Schiff base that effectively inhibited the decomposition of the substrate and formed a dense char at elevated temperatures. The glass transition temperature (T_g) of thermosetting resin is mainly determined by the chemical structure of formulations and the cross-linking density of the network. Thanks to the introduction of more rigid curing agent DDM and network with complete and higher cross-linking density, which compensated for the negative effects of flexible siloxane, the T_g of PTMSi/DDM was slightly lower than that of DGEBA/DDM (Fig. 2b). Similarly, the α transition temperature (T_α) of PTMSi/DDM was consistent with the aforementioned T_g results. From the half-width of tan δ, the uniformity of PTMSi/DDM network was slightly worse than that of DGEBA/DDM. Due to steric hindrance, the uncertainty of the ring-opening curing reaction between reactive epoxide and active hydrogen increased, leading to enhanced fragments participated in the process of α transition in PTMSi/DDM, and increased coordinated movements of the segments in the entire network. In addition, as the temperature continued to rise, a new phase transition appeared in the tanδ curve, which was attributed to the reconstruction of reversible imine bonds, implying the potential reprocessability of PTMSi/DDM (Fig. 2c). A markedly higher storage

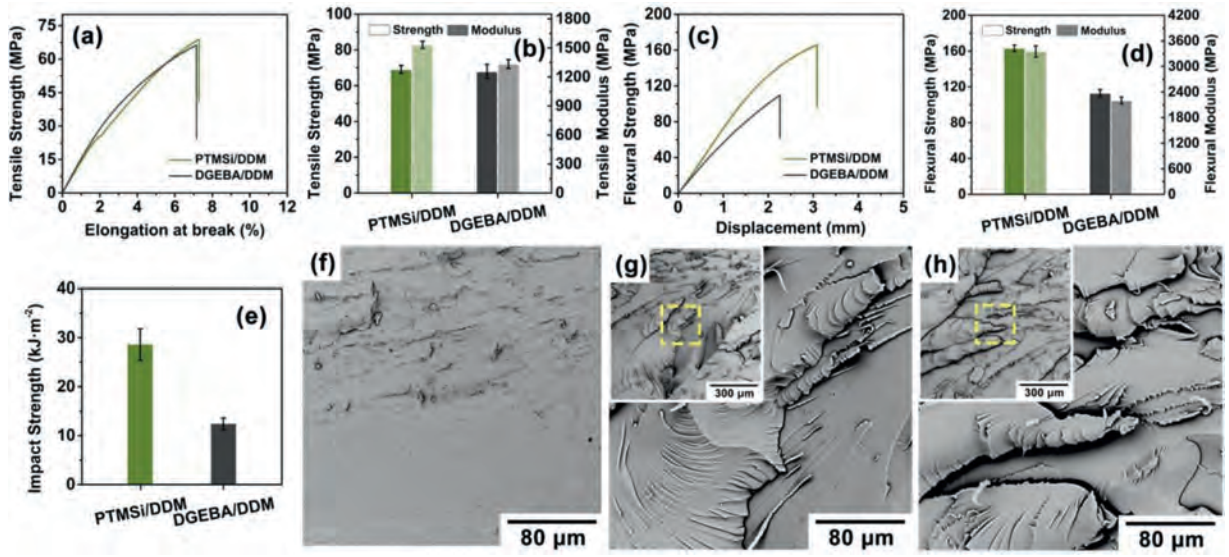

Fig. 3. Mechanical properties of PTMSi/DDM and DGEBA/DDM as a comparison. (a) Stress-strain curves and (b) tensile strength and modulus. (c) Strength-displacement curves and (d) flexural strength and modulus. (e) Unnotched Izod impact strength. SEM images of different morphologies of (f) DGEBA/DDM and (g, h) PTMSi/DDM impact fracture surface, respectively.

modulus (*G'*) was discovered in PTMSi/DDM than DGEBA/DDM at room temperature, and its high rigidity was attributed to the aromatic structure and high cross-linking density (ν_e) in the network. The *G'* curve of PTMSi/DDM in the rubbery platform was significantly higher than that of DGEBA/DDM. The calculated ν_e from the rubbery modulus (E_r) was 3387 mol/m^3, which confirmed its highly cross-linked network (Table S2 in Supporting information).

PTMSi/DDM and DGEBA/DDM showed consistent tensile behaviors (Fig. 3a) and strengths (Fig. 3b). During the test, the specimen fractured directly after reaching the maximum tensile strength. Due to the presence of a great many rigid components and permanent crosslinks in the epoxy networks, only a small amount of deformation occurred before the specimen fracture. The difference was that under a large external force, the frozen segments in PTMSi/DDM network that was plasticized by the flexible siloxane could start to move and stretch, which showed a small inflection point on the stress-strain curve (Fig. 3a). PTMSi/DDM had outstanding and much higher flexural strength and modulus (consistent with the above-mentioned DMA results) than those of DGEBA/DDM (Fig. 3d), indicating that it was a high rigidity and strength epoxy material at room temperature, which benefited from its highly cross-linked network and robust aromatic Schiff base moiety. Since the intermolecular interactions, such as hydrogen bonding that need to be overcome in the direction of flexural test were much higher than those in the direction of tensile test, based on the reference system, the enhancement percentage of the flexural properties was considerably higher than that of the tensile properties (Table S3 in Supporting information). Although the two thermosets exhibited brittle fracture behavior during flexural process, the flexural fracture displacement of PTMSi/DDM was significantly higher than that of DGEBA/DDM (Fig. 3c), implying the fact that the segments in PTMSi/DDM network had a stronger mobility obviously brought from the plasticization of the flexible siloxane. In view of the plastic deformation behavior of PTMSi/DDM found in tensile and flexural tests, which was quite different from that of DGEBA/DDM, the unnotched Izod impact strength was performed to evaluate their impact resistance. Fig. 3e displayed that PTMSi/DDM possessed excellent impact strength, which was significantly higher than that of conventional BPA EPs, and could reach the current level of impact strength of some toughened DGEBA systems [48,49].

The high impact resistance of PTMSi/DDM could be explained by micro morphology of the fracture surface of the specimen after impact test. Different from the smooth and flat fracture surface morphology of DGEBA/DDM (Fig. 3f), the impact fracture surface of PTMSi/DDM exhibited obvious ductile fracture characteristics. A large number of rugged and rough cracks were observed. The directions of the first-level crack and the second-level crack were perpendicular to each other. The second-level crack had a high fold density and "fibrous" fragments were also generated near the fracture section (Figs. 3g and h). All these indicated that the dissipation of fracture energy was promoted through path deflections during the propagation process of impact cracks. Due to the introduction of siloxane significantly improved the flexibility of the network, the mobility of segments enhanced, and so did the toughness of PTMSi/DDM.

As previously discussed, the novel Schiff base-containing EP PTMSi/DDM exhibited excellent comprehensive properties, especially with both high mechanical strengths and toughness, showing obvious advantages over conventional DGEBA resins. In order to specifically evaluate the effect of the rigid and highly cross-linked network on the malleability of the thermoset, the stress relaxation behavior of PTMSi/DDM was analyzed. As shown in Fig. 4a, at a temperature higher than T_g, the relaxation modulus $G(t)/G(0)$ gradually decreased with time and reached a plateau value at 600 s. From the fitting results of relaxation time at different temperatures, the relaxation activation energy (E_a) of PTMSi/DDM was at a low level among that of present Schiff base-containing biobased epoxy CANs (Figs. 4b and d) [24,34,35,50]. Meanwhile, the PTMSi/DDM fragments were able to be reprocessed by hot pressing under certain conditions (Fig. 4c). It showed that the dynamic imine bonds at the film interfaces had a fair contact and diffusion rates, which was mainly because the flexible siloxane increased the mobility of the segments, leading to few restrictions on network topology rearrangements by the stiff network and crosslinks. As can be seen intuitively from the radar map Fig. 4d, PTMSi/DDM did not lose any performances. It not only had comparable or better thermal properties, mechanical strengths and toughness than those of

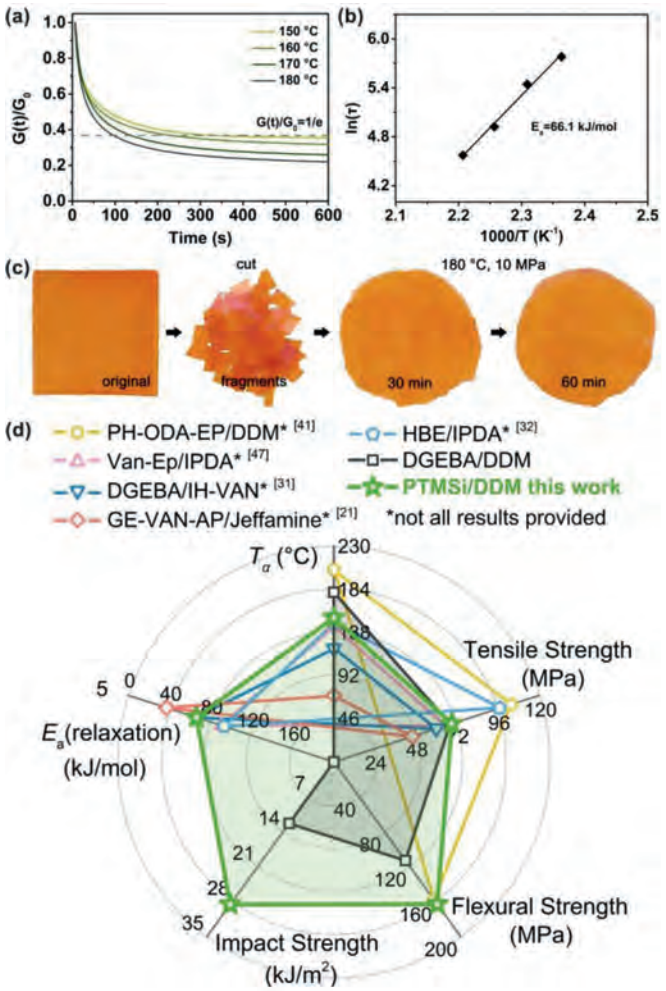

Fig. 4. Malleability of PTMSi/DDM. (a) Normalized relaxation modulus versus time curves at different temperatures. (b) Fitting of the relaxation times to the Arrhenius' equation. (c) Reprocessing experiment. (d) Radar map probing optimal α transition temperature (T_α), mechanical strengths and relaxation activation energy (E_a) of different Schiff base-containing biobased and conventional epoxy resins.

DGEBA/DDM, but also maintained the plasticity of the thermoset, which was relatively rare among Schiff base-containing biobased CANs.

Herein, a novel Schiff base-containing dynamic covalent epoxy thermoset was obtained through a facile aldehyde-amine condensation reaction between biobased protocatechualdehyde and synthetic siloxane-containing amine. Since there were more reactive epoxides in the epoxy monomer than in DGEBA, the cured thermosets possessed high cross-linking density; and the introduction of rigid aromatic Schiff base moieties endowed it with excellent thermal properties, mechanical strength and modulus. On the one hand, the flexible siloxane units improved the impact resistance of the cured product through increasing the chain mobility; on the other hand, it ensured the network topology rearrangements were performed smoothly, and the cured thermosets were malleable. These features provided great potential of the epoxy CAN as an ideal sustainable substitute for bisphenol A epoxy resin for versatile applications.

Declaration of competing interest

The authors declare that they have no known competing financial interests or personal relationships that could have appeared to influence the work reported in this paper.

Acknowledgments

Financial supports by the National Science Foundation of China (Nos. 51822304, 51773137), the 111 Project (No. B20001) and Fundamental Research Funds for the Central Universities are sincerely acknowledged.

Supplementary materials

Supplementary material associated with this article can be found, in the online version, at doi:10.1016/j.cclet.2021.10.079.

References

[1] T. Vidil, F. Tournilhac, S. Musso, et al., Prog. Polym. Sci. 62 (2016) 126–179.
[2] Y.F. Lei, X.L. Wang, B.W. Liu, et al., Chin. Chem. Lett. 32 (2021) 875–879.
[3] Y.F. Lei, X.L. Wang, B.W. Liu, et al., ACS Sustain. Chem. Eng. 8 (2020) 13261–13270.
[4] X.M. Ding, L. Chen, D.M. Guo, et al., ACS Sustain. Chem. Eng. 9 (2021) 3267–3277.
[5] R. Auvergne, S. Caillol, G. David, et al., Chem. Rev. 114 (2014) 1082–1115.
[6] J.R. Rochester, Reprod. Toxicol. 42 (2013) 132–155.
[7] D. Chen, K. Kannan, H. Tan, et al., Environ. Sci. Technol. 50 (2016) 5438–5453.
[8] Z.P. Zhang, M.Z. Rong, M.Q. Zhang, Prog. Polym. Sci. 80 (2018) 39–93.
[9] J. Zhang, V.S. Chevali, H. Wang, et al., Compos. B. Eng. 193 (2020) 108053.
[10] Y. Yang, Y. Xu, Y. Ji, et al., Prog. Mater Sci. 120 (2021) 100710.
[11] C.J. Kloxin, C.N. Bowman, Chem. Soc. Rev. 42 (2013) 7161–7173.
[12] D.W.R. Balkenende, R.A. Olson, S. Balog, et al., Macromolecules 49 (2016) 7877–7885.
[13] Z. Hu, D. Zhang, F. Lu, et al., Macromolecules 51 (2018) 5294–5303.
[14] X. Chen, M.A. Dam, K. Ono, et al., Science 295 (2002) 1698–1702.
[15] H. Hou, J. Yin, X. Jiang, Adv. Mater. 28 (2016) 9126–9132.
[16] G.I. Peterson, J. Lee, T.L. Choi, Macromolecules 52 (2019) 9561–9568.
[17] D. Montarnal, M. Capelot, F. Tournilhac, et al., Science 334 (2011) 965–968.
[18] X. Feng, J. Fan, A. Li, et al., ACS Appl. Mater. Interfaces 11 (2019) 16075–16086.
[19] S. Wang, H. Wang, P. Zhang, et al., Mater. Horiz. 8 (2021) 1481–1487.
[20] M. Roettger, T. Domenech, R. van der Weegen, et al., Science 356 (2017) 62–65.
[21] M.O. Saed, A. Gablier, E.M. Terentejv, Adv. Funct. Mater. 30 (2019) 1906458.
[22] A. Ruiz de Luzuriaga, R. Martin, N. Markaide, et al., Mater. Horiz. 3 (2016) 241–247.
[23] H. Si, L. Zhou, Y. Wu, et al., Compos. B. Eng. 199 (2020) 108278.
[24] S. Zhao, M.M. Abu-Omar, Macromolecules 51 (2018) 9816–9824.
[25] P. Taynton, K. Yu, R.K. Shoemaker, et al., Adv. Mater. 26 (2014) 3938–3942.
[26] Z. Zou, C. Zhu, Y. Li, et al., Sci. Adv. 4 (2018) eaaq0508.
[27] L. Zhang, Z. Liu, X. Wu, et al., Adv. Mater. 31 (2019) 1901402.
[28] Y. Chen, P.G. Miller, X. Ding, et al., Adv. Mater. 32 (2020) 2003761.
[29] C.H. Li, C. Wang, C. Keplinger, et al., Nat. Chem. 8 (2016) 618–624.
[30] C. Hao, T. Liu, S. Zhang, et al., Macromolecules 53 (2020) 3110–3118.
[31] H. Liu, H. Zhang, H. Wang, et al., Chem. Eng. J. 368 (2019) 61–70.
[32] X. Li, J. Zhang, L. Zhang, et al., Compos. Commun. 25 (2021) 100754.
[33] S. Wang, S. Ma, Q. Li, et al., Green Chem. 21 (2019) 1484–1497.
[34] H. Memon, H. Liu, M.A. Rashid, et al., Macromolecules 53 (2020) 621–630.
[35] X. Xu, S. Ma, S. Wang, et al., J. Mater. Chem. A 8 (2020) 11261–11274.
[36] X.L. Zhao, Y.Y. Liu, Y. Weng, et al., ACS Sustain. Chem. Eng. 8 (2020) 15020–15029.
[37] J. Wu, X. Yu, H. Zhang, et al., ACS Sustain. Chem. Eng. 8 (2020) 6479–6487.
[38] Y. Tao, L. Fang, M. Dai, et al., Polym. Chem. 11 (2020) 4500–4506.
[39] T. Liu, C. Hao, L. Wang, et al., Macromolecules 50 (2017) 8588–8597.
[40] Y. Oh, K.M. Lee, D. Jung, et al., ACS Macro Lett. 8 (2019) 239–244.
[41] Y. Liu, B. Wang, S. Ma, et al., Eur. Polym. J. 144 (2021) 110236.
[42] T. Liu, S. Zhang, C. Hao, et al., Macromol. Rapid Commun. 40 (2019) 1800889.
[43] Y.Y. Liu, J. He, Y.D. Li, et al., Ind. Crop. Prod. 153 (2020) 112576.
[44] W. Xie, S. Huang, D. Tang, et al., Chem. Eng. J. 394 (2020) 123667.
[45] W. Xie, S. Huang, S. Liu, et al., Chem. Eng. J. 404 (2021) 126598.
[46] X. Xu, S. Ma, J. Wu, et al., J. Mater. Chem. A 7 (2019) 15420–15431.
[47] C. Aouf, C.L. Guernevé, S. Caillol, et al., Tetrahedron 69 (2013) 1345–1353.
[48] X.F. Liu, B.W. Liu, X. Luo, et al., Chem. Eng. J. 380 (2020) 122471.
[49] J. Zhang, X. Mi, S. Chen, et al., Chem. Eng. J. 381 (2020) 122719.
[50] Q. Yu, X. Peng, Y. Wang, et al., Eur. Polym. J. 117 (2019) 55–63.